Electronic Supplementary Information

One-pot In Situ Functionalization of Cellulose in a CO_2 Switchable Solvent for the Fluorescent Detection of Fe^{3+}

Xiaobo Yu [a, b], Yiting Xu [b], Fei Liu [a, b, *], Wei Zhang [b], Yi Sun [b], Yajin Fang [b], Lanyun Fang [c], Xiaofeng He [a], Haining Na [b, *], Jin Zhu [b]

a School of Materials Science and Engineering, Shenyang University of Chemical Technology, 11th Street, Shenyang Economic and Technological Development Zone, Shenyang 110142, China

b Key Laboratory of Bio-based Polymeric Materials Technology and Application of Zhejiang Province, Ningbo Institute of Materials Technology and Engineering, Chinese Academy of Sciences, 1219 Zhongguan West Road, Zhenhai, Ningbo, Zhejiang, 315201, China

c Ningbo Center For Disease Control And Prevention, 237 Yongfeng Road, Haishu, Ningbo, Zhejiang, 315010, China

Xiaobo Yu: yuxiaobo@nimte.ac.cn; Yiting Xu: xuyiting@nimte.ac.cn

Fei Liu: liufei@nimte.ac.cn; Wei Zhang: zhangwei1997@nimte.ac.cn

Yi Sun: sunyi@nimte.ac.cn; Yajin Fang: fangyajin@nimte.ac.cn

Lanyun Fang: 541191064@qq.com; Xiaofeng He: hexiaofeng99063@sina.com

Haining Na: nahaining@nimte.ac.cn; Jin Zhu: jzhu@nimte.ac.cn

* Corresponding Authors:

Dr. Fei Liu, liufei@nimte.ac.cn

Dr. Haining Na, nahaining@nimte.ac.cn

1.Experimental section

Materials

Microcrystalline cellulose (MCC) was dried under vacuum at 80 °C for 12 h before use. Carbon dioxide (CO_2, >99.9%) was purchased from Wanli Gas Co., Ltd (Ningbo, China). 5-Methylsalicylaldehyde (5-MSA, >98%), dimethyl malonate (DMM, >98%), dibenzoyl peroxide (BPO, >99%), and isopropanol (>99.5%) were purchased from Shanghai Macklin Biochemical Technology Co. L-Proline (>99%), dimethyl sulfoxide (DMSO, >99.8%), N, N-dimethylacetamide (DMAc, >99.9%), dichloromethane (DCM, >99.5%), chloroform (>99%), ethanol (>99%), methanol (>99.5%), 1,8-diazabicyclo[5.4.0]undec-7-ene (DBU, >99%), N-Bromosuccinimide (NBS, >99%), and L-lactide (LA, >98%, (Mn = 66 kDa, Mw = 178 kDa)) were purchased from Shanghai Aladdin Biochemical Technology Co. Ltd. All reagents were used as received without further purification.

Synthesis of Fluorescent Cellulose

In the first step, MCC (0.47 g, 3.0 mmol,), DMSO (10 g, 9.1 mL), and DBU (1.4 g, 9.0 mmol) were added to a 250 mL stainless steel reactor, where the molar ratio of DBU to anhydrous glucose unit (AGU) was 3:1. The reactor was closed, and the temperature was gradually increased to 55 ^{o}C. CO_2 was continuously introduced, and mechanical stirring was maintained for 2 h. When the reaction was completed, a homogeneous, clear, transparent, and light yellow cellulose solution with a concentration of 4.0 wt% was obtained.

Subsequently, LA (6.912 g, 48 mmol) was added to the obtained cellulose solution, and the reaction was mechanically stirred for 8 h at 80 ^{o}C under a nitrogen atmosphere, where the molar ratio of AGU to LA was 1:16. The mixture was cooled to room temperature after completion. C-*g*-PLLA (Mn = 66 kDa and Mw = 178 kDa).[1]

Finally, 6-BrMCM (0.8910 g, 3.0 mmol) was added to the above homogeneous solution, where C-*g*-PLLA was fabricated. The reaction was carried out at 30 °C under 0.8 MPa CO_2 pressure with mechanical stirring for 4 h. After the reaction was completed, the mixture was washed three times by settling with methanol and then poured into isopropanol (100 mL). Afterward, the resulting solid product was dried in a vacuum oven at 80 °C for 24 h to obtain the final product C-*g*-PLLA/MCD.

Preparation of nanofibrous film by electrostatic spinning

C-*g*-PLLA/MCD (8.0 g) was dissolved in a mixture of acetone and DMAc (6g, w/w 1:1). A homogeneous solution with a C-*g*-PLLA/MCD concentration of 57.14 wt% was obtained for the subsequent electrostatic spinning. The solution was put into a 5 mL syringe, and electrostatic spinning was carried out at a voltage of 20 kV with a jet speed of 2.0 mL/h. The distance from the needle tip to the roller was about 10 cm, the roller speed was 84 rad/min^{-1}, and the nanofibrous film was obtained after about 3 h. The power supply was DW-P503-1ACDF AC high-voltage power source, and the injection pump is TJ-3A of Baoding Lange Co.

Characterization

The proton NMR spectrum (^{1}H NMR) was tested using a Bruker AVANCE III 600 MHz NMR instrument with DMSO-*d*6 as the solvent and TMS (Tetramethylsilane) as the internal standard, and the carbon thirteen NMR spectrum was tested using a Bruker AVANCE III 600 MHz NMR instrument with DMSO-*d*6 as solvent (^{13}C NMR). The degree of substitution of MCD (DS_{MCD}), PLLA (DS_{PLLA}) in the synthesized C-*g*-PLLA/MCD, the degree of polymerization (DP_{PLLA}), the molar degree of substitution (MS_{PLLA}), and the weight content of PLLA (W_{PLLA}) can be calculated according to the following equations:[2–5]

$$DP_{PLLA}=(I_{A'}+I_A)/I_{A'} \quad (1)$$

$$DS_{PLLA}=I_{A'}/(I_{(3.0\text{-}5.5)}-I_{(3.3)}-I_{(B)}-I_{(B')}) \quad (2)$$

$$MS_{PLLA}=DP\times DS \quad (3)$$

$$W_{PLLA}=72MS/(162+72MS) \quad (4)$$

$$DS_{MCD}=7I_{MCD}/17(I_{(3.0\text{-}5.5)}-I_{(3.3)}-I_{(B)}-I_{(B')}-I_{(k,g,f,e)}) \quad (5)$$

I_A, $I_{A'}$, $I_{(B)}$, and $I_{(B')}$ are the (A), (A'), (B), and (B') proton peak intensities, respectively, I_{MCD} and $I_{(3.0\text{-}5.5)}$ are the proton peak intensities of MCD and AGU, $I_{(k,g,f,e)}$ is the proton peak intensity of MCD in AGU and 72 and 162 are the molecular weights of lactic acid-based units and AGU, respectively.

Fourier transforms infrared (FT-IR) testing was performed with a Nicolet 6700 infrared spectrometer using potassium bromide (KBr) pressed samples with spectra in the 4000-400 cm^{-1} range and a total of 16 scans per sample.

Thermogravimetric analysis (TGA) was performed using a Diamond TGA/DTA1 thermogravimetric analyzer. The measurements were performed under a nitrogen-protected atmosphere, and its ramp-up rate was set at 20 °C·min^{-1} with a temperature range of 50-800 °C.

The differential scanning calorimetry (DSC) analysis was performed on a NETZSCH DSC214 instrument, calibrated with an indium standard, and the measurements were performed under a nitrogen-protected atmosphere. First, the sample was heated to 220 °C at a rate of 10 °C·min^{-1} and held at 220 °C for 5 min to eliminate thermal history, then cooled to -40°C at a rate of 10 °C·min^{-1}. The second heating range was -40-220 °C with the same heating rate of 10 °C·min^{-1} as the first heating. The second heating curve determined all glass transition temperatures (T_g).

The mass spectrometry was performed using an Agilent Gas Chromatograph (7890B-5977A) for its relative molecular mass.

Ultraviolet absorption (UV-Vis) was measured using an ultraviolet-visible near-

infrared spectrophotometer (LAMBDA 950) with a wavelength range set to 800-200 nm.

The fluorescence emission wavelength was measured in the range of 380-710 nm using a xenon (Xe) 150W fluorescence spectrometer (FL3-111), and the fluorescence excitation slit width was set to 2/5 nm and the excitation wavelength to 365 nm. And the time-resolved fluorescence spectra can be tested.

X-ray diffraction (XRD) was measured using a D8 ADVANCE X-ray diffractometer with a diffraction intensity measurement range between 2θ=5-60°.

Polarized light microscopy (POM, BX51) analysis was used to detect samples' melting and flowing process in the 50-300 °C temperature range.

A superheated field emission scanning electron microscope (SEM) Verios G4 UC was used to observe the surface morphology of the nanofibrous films in nitrogen, and the samples were all subjected to approximately 120 s of 10 nm Pt sputtering on the surface using an anion sputter coater (E-1045, Hitachi) before testing.

Biotype laser confocal microscope (LEICA) TCS SP5 was used to observe the fluorescence properties of filamentous fibers in nanofibrous membranes.

The Japanese Otsuka QE-2100 quantum efficiency tester conducted the quantum efficiency test.

The X-ray photoelectron spectrometer (XPS) uses AXIS SUPRA to test the binding energy of fluorescent materials.

2. Supplementary figures and tables

Synthesis of methyl 6-methyl coumarin-3-carboxylate (6-MCM)

The 6-MCM was synthesized according to the literature[6,7] 5-MSA (408.0 mg, 3 mmol) and DMM (396.0 mg, 3 mmol) were mixed in a round bottom flask and L-proline (34.5 mg, 10 mol% of 5-MSA) was added as catalyst. The mixture was heated to 80 °C and reacted for 0.5 h. When the reaction was completed, the mixture was cooled to room temperature and then recrystallized in ethanol to give 6-MCM in a white powder with a high yield of 88%.^{1}H NMR (600 MHz, DMSO-*d*6): δ(TMS, ppm) 8.69 (s, 1H),7.68 (s, 1H), 7.56 (dd, *J* = 8.5, 2.3 Hz, 1H), 7.33 (d, *J* = 8.7 Hz, 1H), 3.84 (d, *J* = 1.7 Hz, 3H), 2.37 (s, 3H).

Synthesis of 6-bromomethyl coumarin-3-carboxylic acid methyl ester (6-BrMCM)

6-BrMCM was synthesized according to a previous study.[4] 6-MCM (0.545 g, 2.5 mmol) and NBS (0.445 g, 2.5 mmol) were added to a flask containing 50 mL of chloroform. The mixture was stirred for 30 min at room temperature and then BPO (10.8 mg, 0.0445 mmol) was added as initiator. The reaction was carried out at 64 °C for 12 h. When the reaction was completed, the mixture was washed with brine and dried with anhydrous magnesium sulfate. The organic phase was separated and then subjected to rotary evaporation to remove the solvent to give the crude product, which was then recrystallized from ethanol. The product was treated with flash silica gel (ethyl acetate/petroleum ether = 1:2) and the resulting yield was 39%. [8] ^{1}H NMR (600 MHz, DMSO-*d*6): *δ* 8.76 (s, 1H), 7.99 (d, *J* = 2.3 Hz, 1H),7.81 (dd, *J* = 8.6, 2.2 Hz, 1H), 7.45 (d, *J* = 8.5 Hz, 1H), 4.79 (s, 2H), 3.84 (s, 3H).

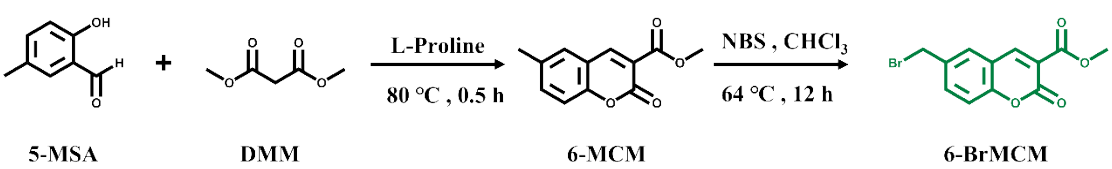

Scheme S1. Synthesis of 6-MCM and 6-BrMCM.

Synthesis of MCD

The product MCD was obtained by using 6-MCM (2.18 g, 10 mmol) with DBU (0.76 g, 5 mmol) at 30 °C for 4 h under mechanical stirring at 0.8 MPa CO_2 or under atmosphere pressure or heating at 120-130 °C under atmosphere pressure for 2 h, followed by washing with ether and isopropanol.[9,10]

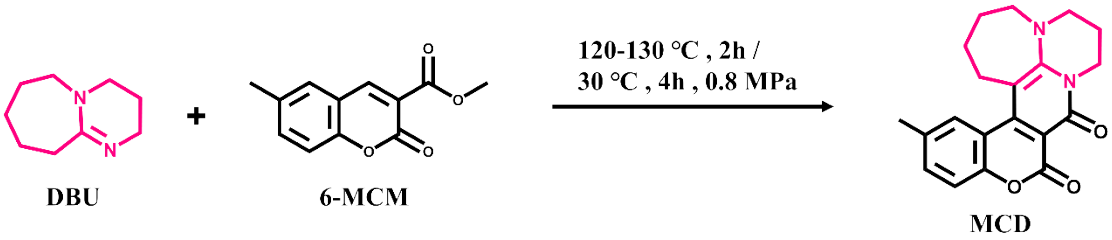

Scheme S2. Synthesis of MCD.

Preparation of C-*g*-PLLA/MCD+Fe^{3+} samples for FT-IR spectroscopy

To determine the location of the complexes of C-*g*-PLLA/MCD with Fe^{3+}, the IR spectra of C-*g*-PLLA/MCD with Fe^{3+} were analyzed and compared. The sample of C-*g*-PLLA/MCD+Fe^{3+} used for FT-IR spectroscopy was made by adding 200 μL of Fe^{3+} aqueous solution (20 mM) to DMSO solution of C-*g*-PLLA/MCD, stirring for 10 min and then removing the solvent and drying.

Structure of 6-MCM

6-MCM was prepared according to the synthetic route of Scheme S1. FT-IR spectra of methyl 6-methyl coumarin-3-carboxylate (6-MCM) are given in Figure S1(a), from which it can be seen that the curve of 6-MCM shows a stretching vibration peak of C=C double bond on the unsaturated carbon atom at 3066 cm^{-1}, a stretching C=O at 1757 cm^{-1} vibration peak, indicating the formation of the ester group, a stretching vibration peak of C-CH_3 at 1380 cm^{-1}, proving the formation of the methyl group at the 6-position of coumarin derivative, and a stretching vibration peak of C-O-C at 1150-1300 cm^{-1}, thus further proving, the formation of methyl ester of

carboxylic acid at the 3-position, thus proving the successful synthesis of 6-MCM. [11]

The NMR hydrogen spectra (^{1}H-NMR) of 6-MCM are shown in Figure S1 (b), with DMSO-*d*6 as the solvent, and the chemical shifts (δ) of the methyl group on coumarin 6-position at 2.44 ppm (*f*), methyl group on coumarin 4 carboxylic acid methyl ester at 3.97 ppm (*e*), H on benzene ring at 7.24-7.52 ppm (*b*-*d*) displacement, and 8.52 ppm (*a*) was the chemical shift of H at the 4-position of coumarin, thus proving the successful synthesis of 6-MCM.

The nuclear magnetic resonance carbon spectrum (13C-NMR) of 6-MCM is shown in Figure S1 (c). 21.7ppm is the chemical shift (δ) of methyl at the 6 sites of coumarin, 52.0ppm is the chemical shift of methyl C at the 4 sites of carboxylate methyl coumarin, and 114.3-155.7ppm is the chemical shift of C at the 4 sites of coumarin. At 165ppm, the chemical shift of ester group C on the 4 carboxylate methyl esters of coumarin further proves the successful synthesis of 6-MCM.

It can be seen from the time-of-flight mass spectrum in Figure S1 (d) that the mass charge ratio of 6-MCM is m/z (%) 220[m+H^++1], 219[m+H^+], thus proving the successful synthesis of 6-MCM.

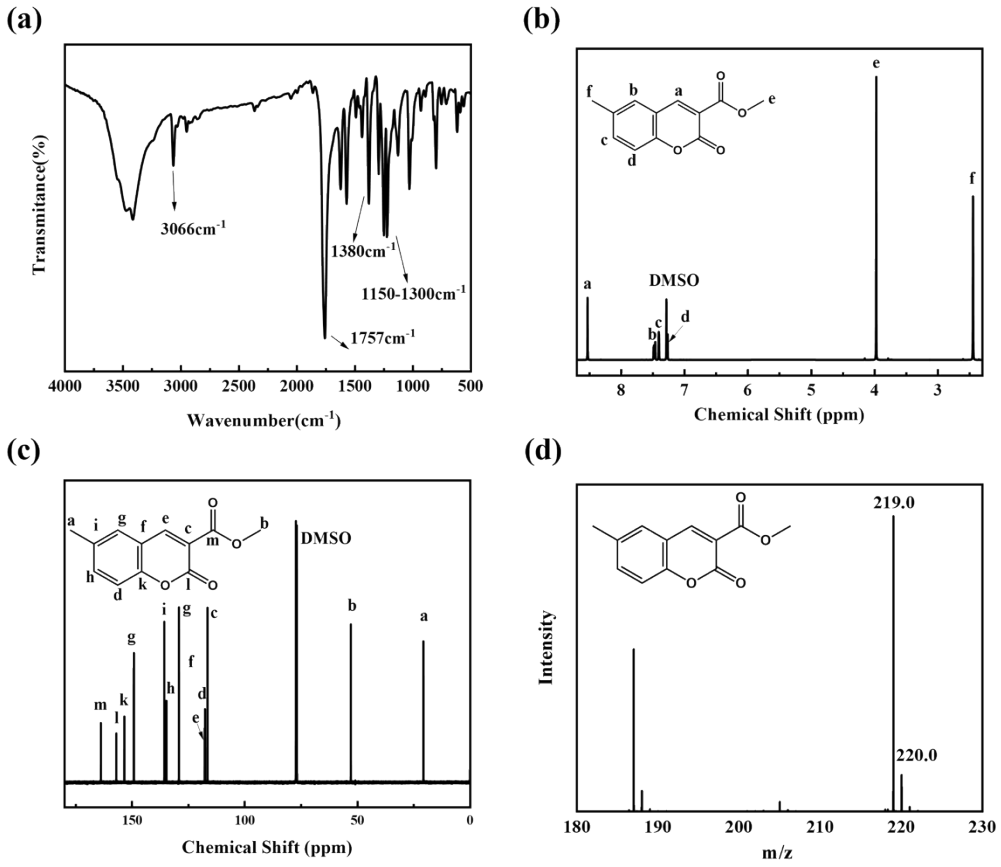

Figure S1. (a) FT-IR, (b) ^{1}H-NMR, (c) ^{13}C-NMR, and (d) mass spectra of 6-MCM.

Structure of 6-BrMCM

Figure S2 (a) gives the FT-IR spectrum of 6-Bromomethyl coumarin-3-carboxylic acid methyl ester (6-BrMCM), from which it can be seen that the curve of 6-BrMCM still retains the stretching vibration peak of the C=C double bond on the unsaturated carbon atom at 3064 cm^{-1}, and the stretching vibration peak of C=O at 1750 $cm^{-1,}$ which indicates that the ester group still exists. The stretching vibration peak of the benzene ring skeleton at 1573 cm^{-1} and the new stretching vibration peak of -CH_2- at 2950 cm^{-1} proved that the methyl group at the 6-position of the coumarin derivative had been converted to methylene group, further proving the successful completion of the bromination at the 6-position methyl group, and therefore the successful synthesis of 6-BrMCM.

The NMR hydrogen spectrum (^{1}H-NMR) of 6-BrMCM is shown in Figure S2(b),

with DMSO-*d*6 as the solvent, at 3.84 ppm (f) for the chemical shift of methyl group on the methyl ester of carboxylic acid at position 4 of coumarin, 4.79 ppm (e) for the chemical shift of methylene group at position 6, 8.76 ppm (a) for the chemical shift of H at position 4 of coumarin, and 6 The disappearance of the methyl group at the 6 position and the formation of the methylene group further proved the successful synthesis of 6-BrMCM.

The nuclear magnetic resonance carbon spectrum (^{13}C-NMR) of 6-BrMCM is shown in Figure S2 (c). 33.54ppm is the chemical shift of methylene at coumarin 6, 52.97 ppm is the chemical shift of methyl C at coumarin 4 carboxylate methyl, and 117.24-156.30 ppm is the chemical shift of C at coumarin. At 163.54ppm, the chemical shift of ester group C on the 4 sites of coumarin carboxylate methyl ester was obtained, which further proved the successful synthesis of 6-BrMCM by NMR carbon spectroscopy.

It can be seen from the time-of-flight mass spectrum in Figure S2 (d) that the mass charge ratio of 6-BrMCM is m/z (%) 298.9[m+H^++1] and 296.9[m+H^+-1], which proves the successful synthesis of 6-BrMCM.

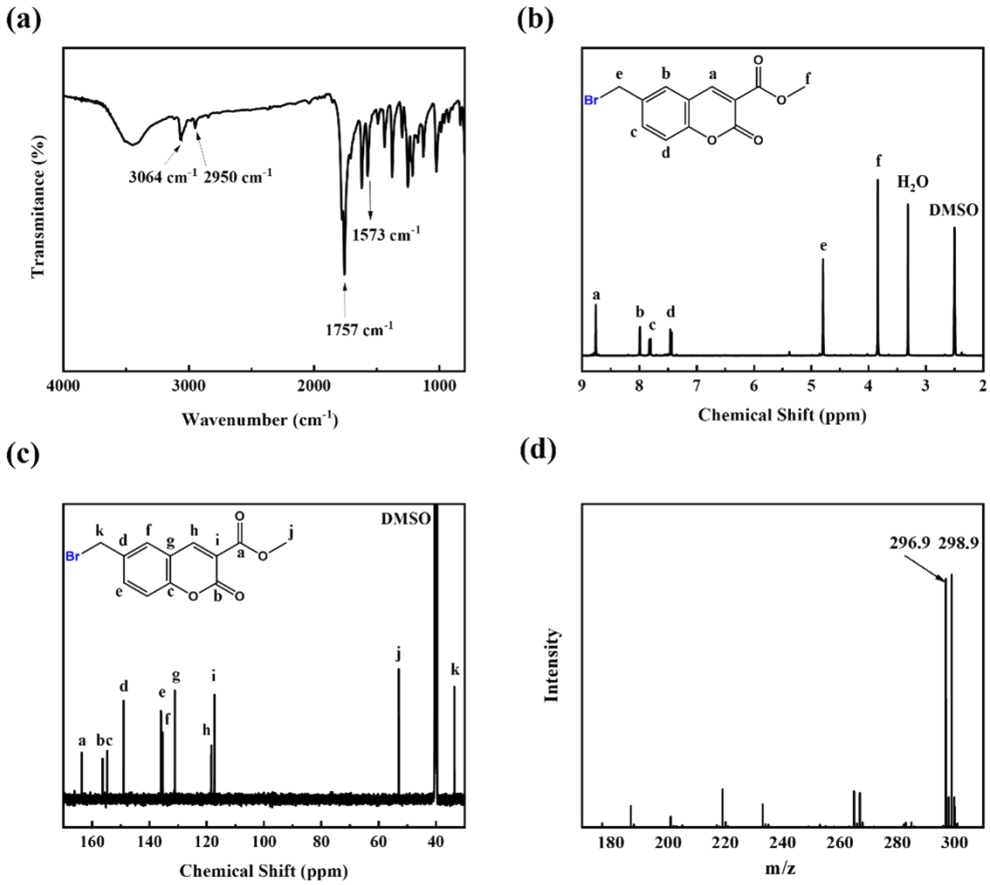

Figure S2. (a) FT-IR, (b) ^{1}H-NMR, (c) ^{13}C-NMR, and (d) Mass spectra of 6-BrMCM.

Structure of MCD

The nuclear magnetic resonance hydrogen spectrum (^{1}H-NMR) of MCD is shown in Figure S3(a), and the crude product of MCD was recrystallized from EtOH using DMSO-*d*6 as solvent. The yield was 65%.^{1}H NMR (600 MHz, DMSO- *d*6): δ (TMS, ppm) 7.76 (s, 1H), 7.31 (dd, *J* = 8.3, 1.9 Hz, 1H), 7.09 (d, *J* = 8.3 Hz, 1H), 3.98 (s, 2H), 3.66 (s, 2H), 3.39 (t, *J* = 6.5 Hz, 2H), 2.33 (s, 3H), 1.99 (p, *J* = 6.0 Hz, 2H), 1.90 (p, *J* = 6.3 Hz, 2H), 1.76 (p, *J* = 6.2 Hz, 2H). This can prove the successful synthesis of MCD. For different reaction conditions, we found that MCD could be synthesized at 120 °C for 2 h and 30°C for 4 h at 0.8 MPa, but only at 30 °C for 4 h at 0.1 MPa, and the fluorescence emission spectrum was shown in Figure S3(b).

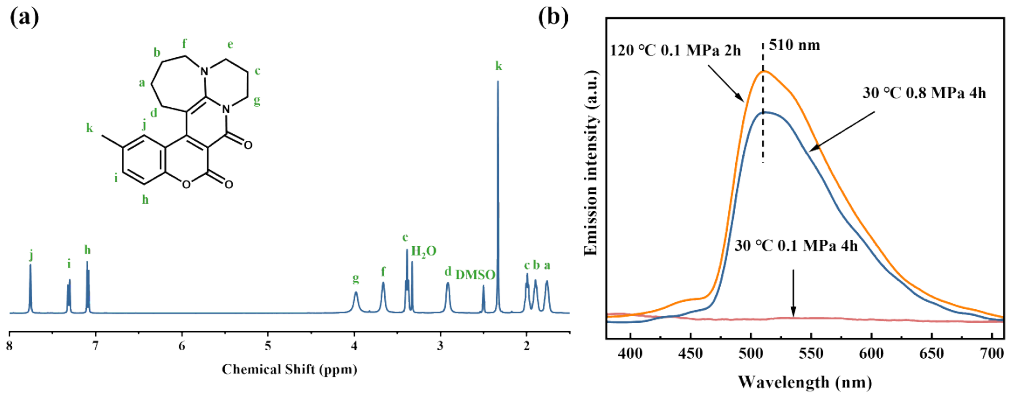

Figure S3. (a) NMR spectra of MCD and (b) fluorescence emission spectra of MCD in DMSO solution (60 mg/mL) obtained after the reaction under different conditions.

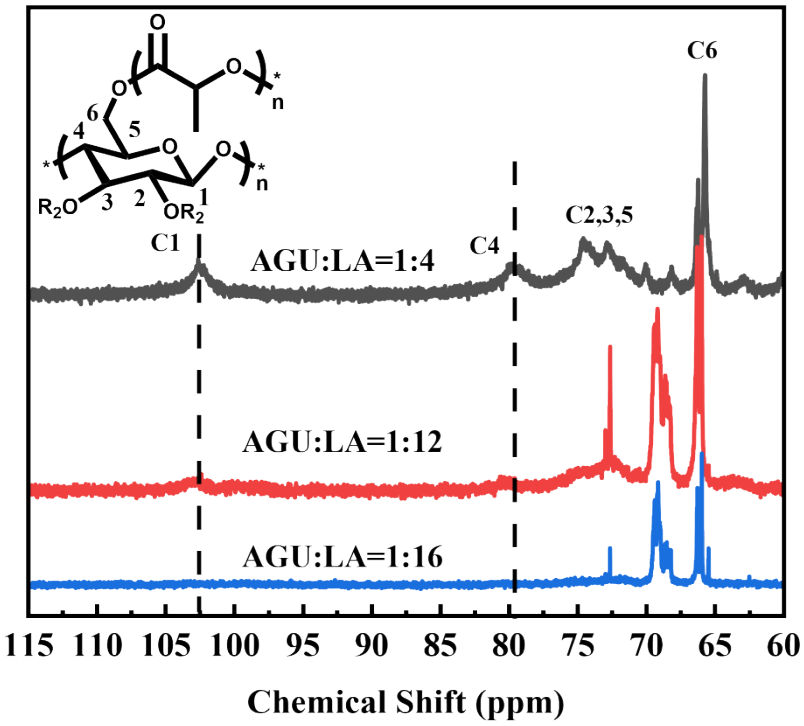

Figure S4. ^{13}C NMR spectra of C-*g*-PLLA with different feed ratios of AGU and LA.

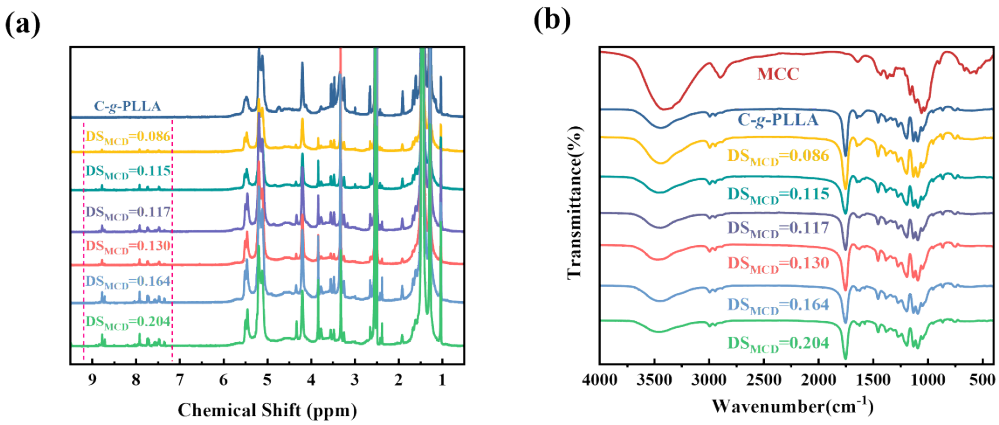

Figure S5. (a) ^{1}H NMR and (b) FT-IR spectra of MCC, C-*g*-PLLA, and C-*g*-PLLA/MCD with different DS_{MCD}.

Table S1. Chemical structure and thermal properties of C-*g*-PLLA/MCD.

No.	Molar ratio of 6-BrMCM/AGU	DS_{PLLA}	DP_{PLLA}	MS_{PLLA}	W_{PLLA}	DS_{MCD}	T_g (°C)	$T_{5\%}$ (°C)	$T_{d,\,max}$ (°C)
1	1.0	1.42	3.86	5.48	0.71	0.086	44.52	269.9	289.7
2	1.5	1.47	3.81	5.60	0.71	0.115	45.85	273.8	280.8
3	2.0	1.58	3.68	5.81	0.72	0.117	46.05	277.1	295.8
4	2.5	1.70	3.96	6.73	0.75	0.130	47.22	287.8	308.2
5	3.0	1.54	3.48	5.92	0.72	0.164	49.82	275.2	297.2
6	4.0	1.50	3.90	5.85	0.72	0.204	49.20	282.4	301.3

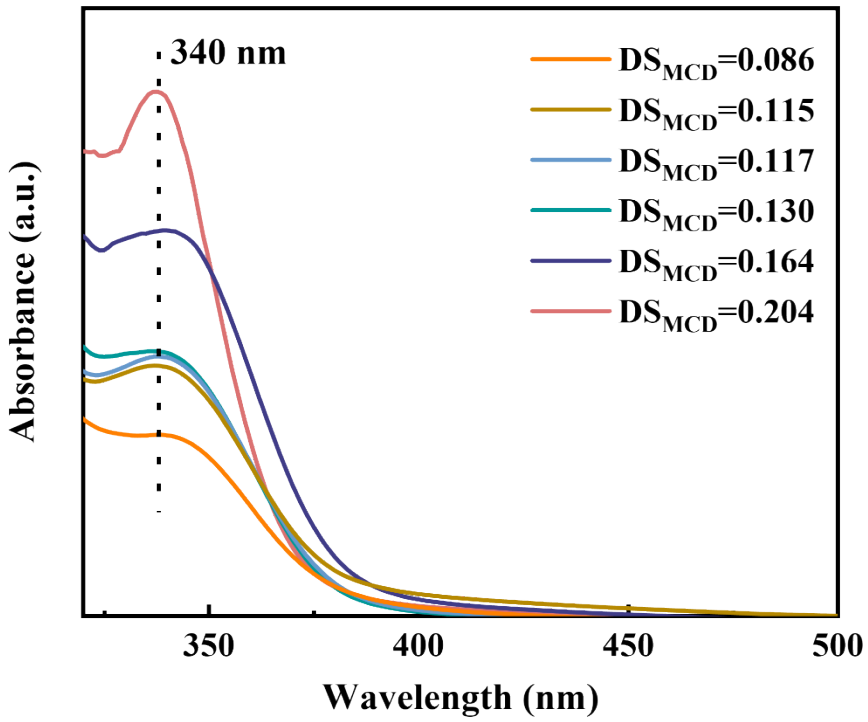

Figure S6. UV-Vis absorption spectra of C-*g*-PLLA/MCD with different DS_{MCD}.

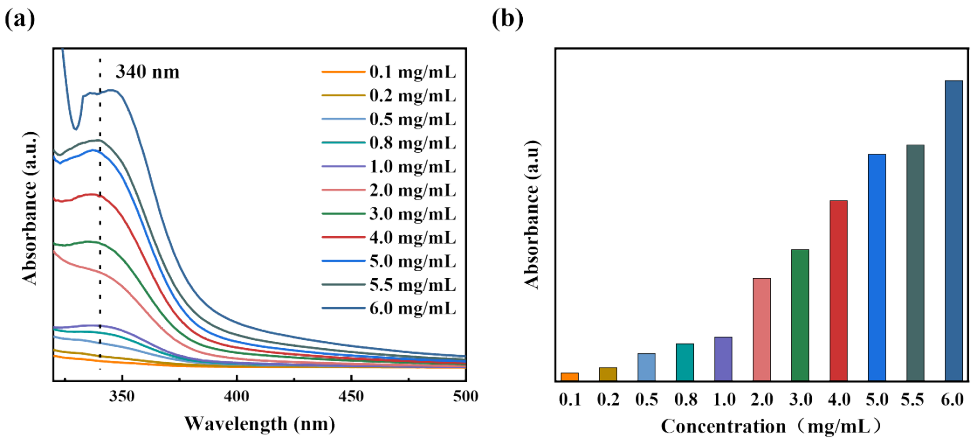

Figure S7. (a) UV-Vis absorption spectra of C-*g*-PLLA/MCD solution at different concentrations, (b) intensity of absorbance at 340 nm of C-*g*-PLLA/MCD solution at different concentrations.

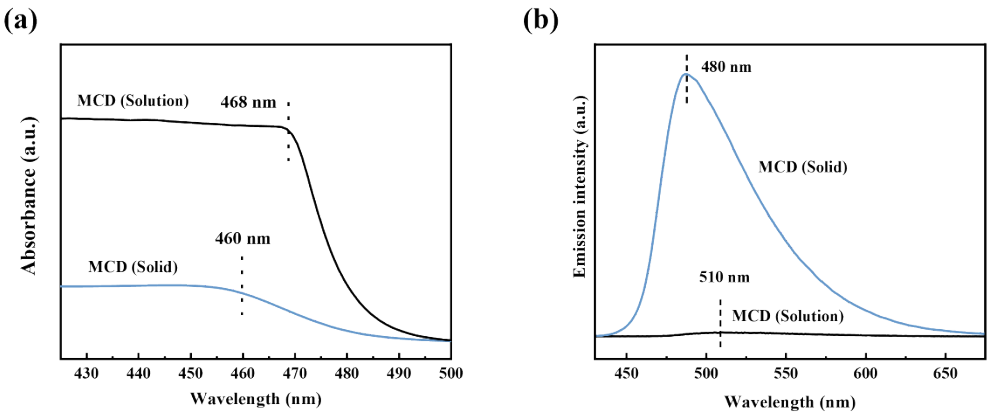

Figure S8. (a) UV absorption spectra and (b) fluorescence emission spectra of MCD solid sample and solution in DMSO (60 mg/mL).

Figure S9. With the evaporation of the solvent of MCD solution (dissolved in ethanol), "N" appears under UV light.

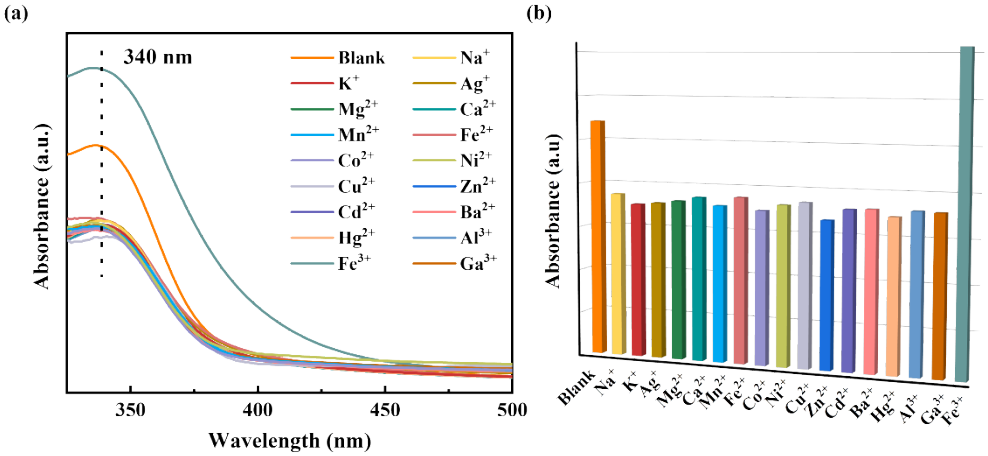

Figure S10. (a) UV-Vis absorption, and (b) intensity of absorbance at 340 nm, of C-*g*-PLLA/MCD solution in DMSO under visible and UV lights upon interaction with

different metal ions [$M(Cl)_x$].

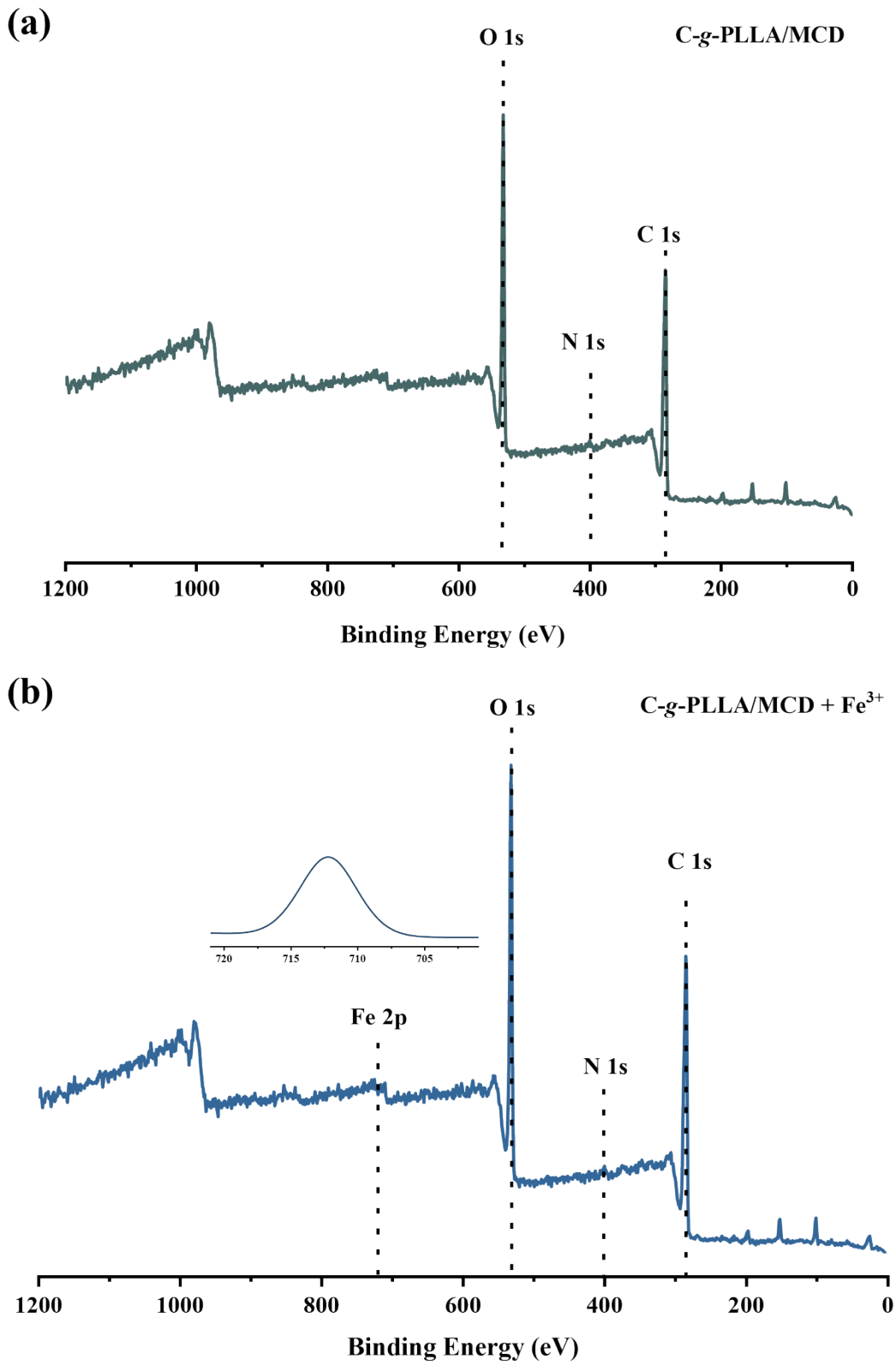

Figure S11. XPS of (a) C-*g*-PLLA/MCD and (b) C-*g*-PLLA/MCD+Fe^{3+}.

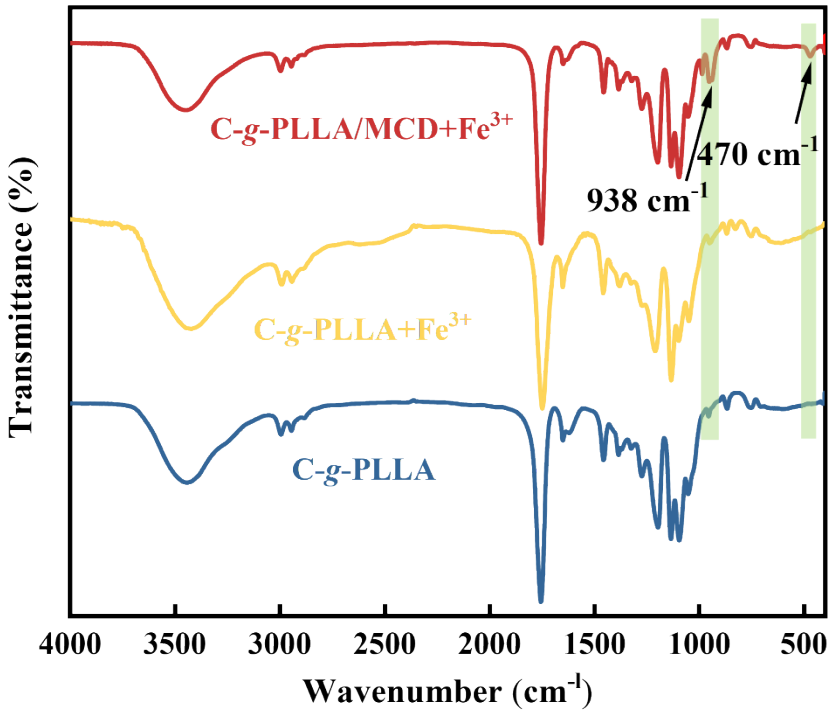

Figure S12. FT-IR spectra of C-*g*-PLLA/MCD+Fe^{3+}, C-*g*-PLLA+Fe^{3+}, and C-*g*-PLLA.

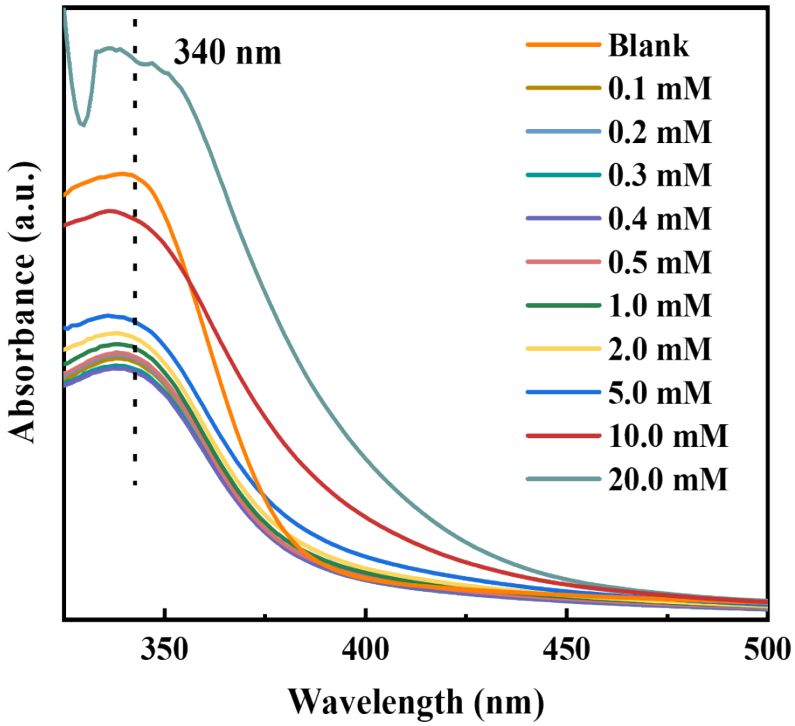

Figure S13. UV-Vis absorbance spectra of C-*g*-PLLA/MCD solution with different concentrations of Fe^{3+}.

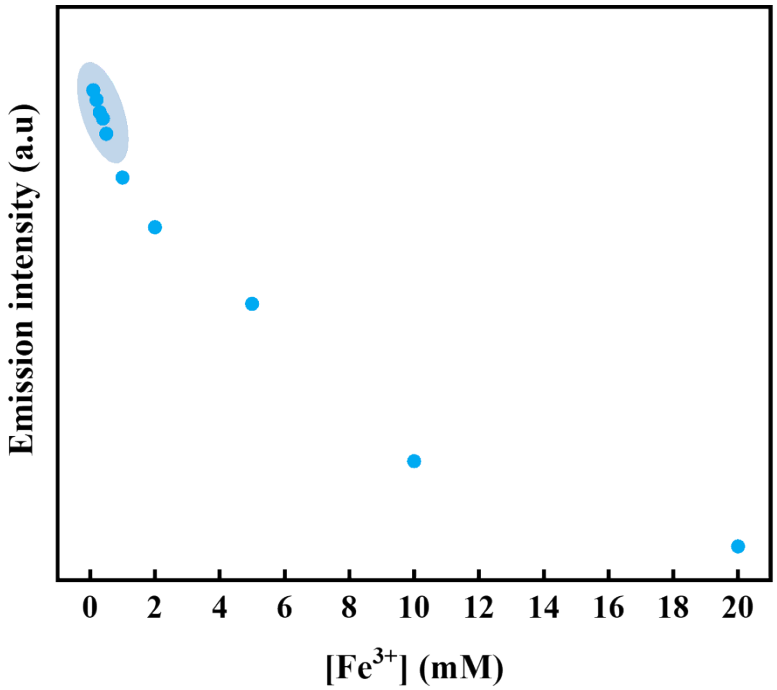

Figure S14. Fluorescence emission peak intensity of C-*g*-PLLA/MCD solution at 430 nm with respect to Fe^{3+} concentrations.

Table S2. Measurements of Fe^{3+} in different water samples.

Samples	Spiked (μM)	Detected (μM)	Recovery (%)	RSD (%, n=3)
Tap water	0	No detected	-	-
	10	10.53±0.52	105.30	5.20
	20	19.79±0.35	98.95	1.73
	30	29.51±0.29	98.37	0.97
	40	40.44±0.99	101.10	2.48
Mineral water	0	No detected	-	-
	10	10.45±0.35	104.50	3.50
	20	19.76±0.33	98.80	1.65
	30	30.40±0.52	101.33	1.73
	40	40.17±0.72	100.42	1.81

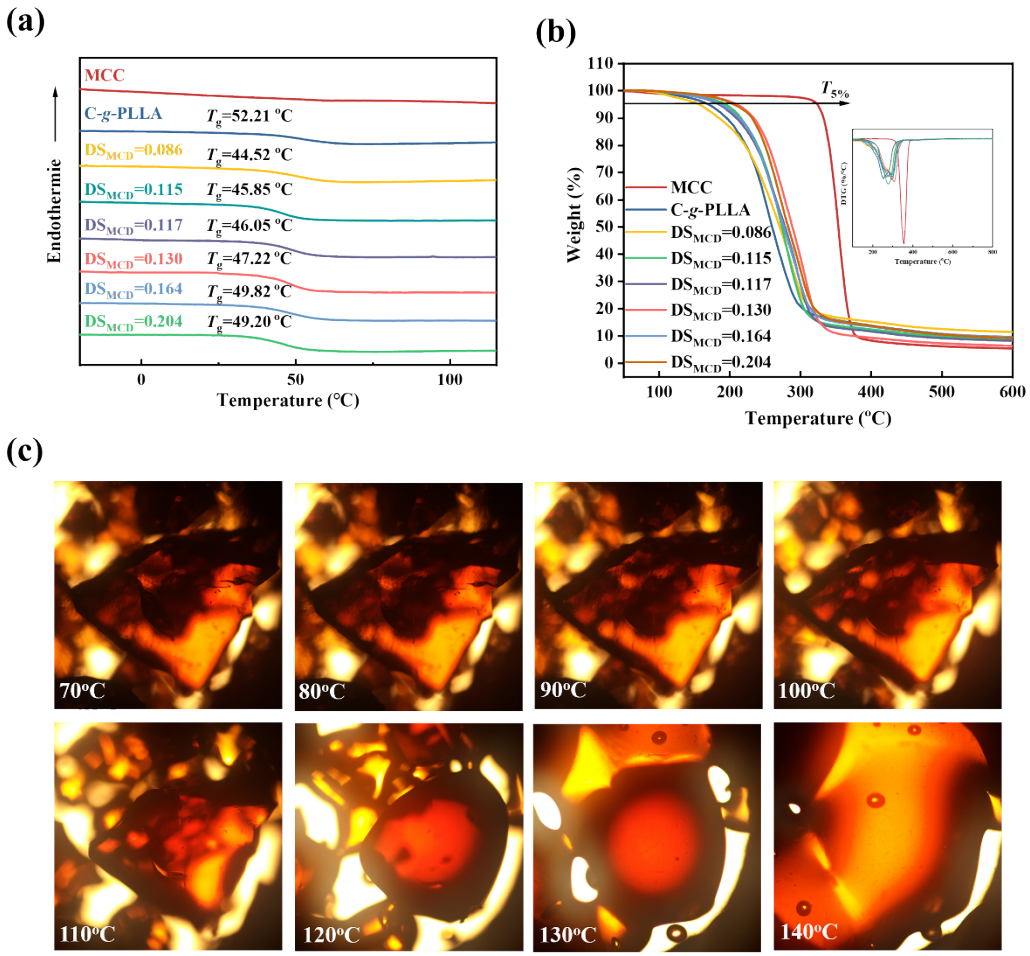

Figure S15. (a) DSC and (b) TGA curves of MCC, C-*g*-PLLA, and C-*g*-PLLA/MCD, and (c) POM images of C-*g*-PLLA/MCD (DS_{MCD}=0.086) at different temperatures.

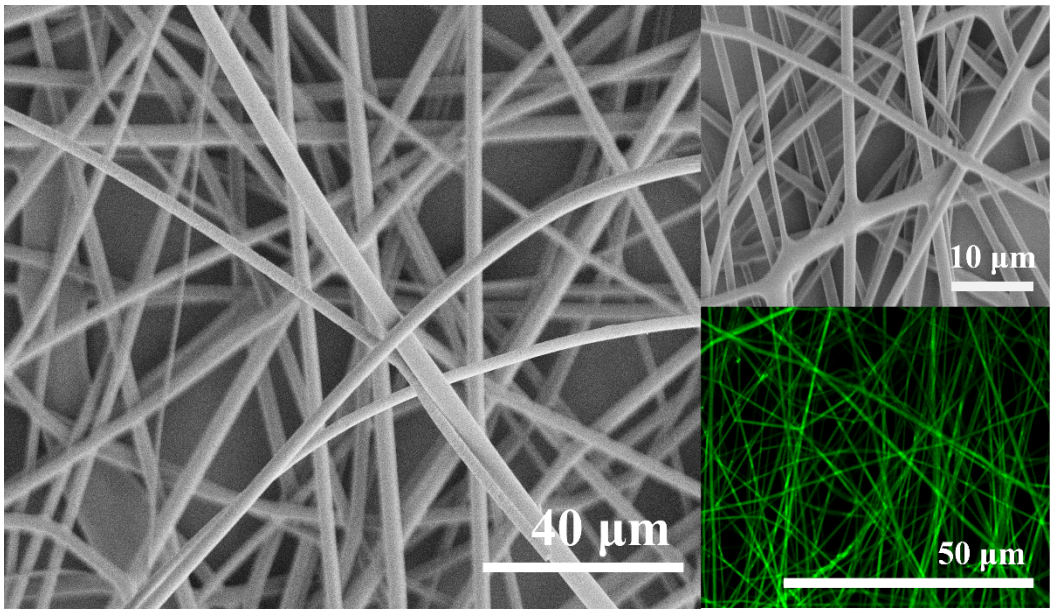

Figure S16. SEM and CLSM images of C-*g*-PLLA/MCD nanofibrous film.

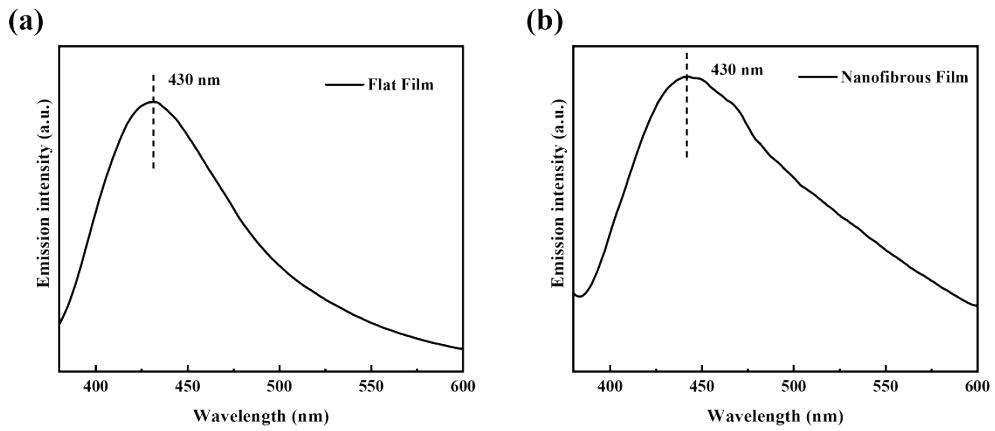

Figure S17. (a) Fluorescent emission spectra of flat films and (b) nanofiber films

Application of the flat film as a smart tag for the qualitative detection and the real-time and dynamic monitoring of Fe^{3+} in water flow：

See recorded video.

References

1 S. Lu, J. Li, F. Liu, M. Chen, H. Na and J. Zhu, *Polymer (Guildf).*, 2021, **229**, 124020.

2 Z. Yao, S. Mi, B. Chen, F. Liu, H. Na and J. Zhu, *ACS Sustain. Chem. Eng.*, 2022, **10**, 17327–17335.

3 S. Mi, Z. Yao, F. Liu, Y. Li, J. Wang, H. Na and J. Zhu, *Green Chem.*, 2022, **24**, 8677–8684.

4 W. Zhang, Y. Sun, Y. Xu, X. Yu, Y. Fang, F. Liu, H. Na and J. Zhu, *Macromol. Chem. Phys.*, , DOI:10.1002/macp.202300036.

5 Y. Sun, W. Zhang, S. Lu, W. Miao, M. Chen, F. Liu, H. Na and J. Zhu, *Carbohydr. Polym.*, 2023, **301**, 120346.

6 D. I. Bugaenko, A. V. Karchava, Z. A. Yunusova and M. A. Yurovskaya, *Chem. Heterocycl. Compd.*, 2019, 55, 483–489.

7 N. N. * Karade, S. V Gampawar, S. V. B. Shinde and W. N. Jadhav, *L-Proline Catalyzed Solvent-Free Knoevenagel Condensation for the Synthesis of 3-Substituted Coumarins*, 2007, vol. 25.

8 C. H. M. Amijs, G. P. M. Van Klink and G. Van Koten, *Green Chem.*, 2003, **5**, 470–474.

9 F. Bu, R. Duan, Y. Xie, Y. Yi, Q. Peng, R. Hu, A. Qin, Z. Zhao and B. Z. Tang, *Angew. Chemie*, 2015, **127**, 14700–14705.

10 Y. M. Poronik and D. T. Gryko, *Chem. Commun.*, 2014, **50**, 5688–5690.

11 P. Verdía, F. Santamarta and E. Tojo, *Molecules*, 2011, **16**, 4379–4388.